Energy

FOSSIL

DOE/LC/10650-T1
(DE84006251)

THE OXIDATION/GASIFICATION OF CARBON RESIDUE ON RETORTED OIL SHALE

Final Report

By
William J. Thomson

January 16, 1984

Work Performed Under Contract No. AT20-81LC10650

Washington State University
Pullman, Washington

Technical Information Center
Office of Scientific and Technical Information
United States Department of Energy

DISCLAIMER

DISCLAIMER

This report has been reproduced directly from the best available copy.

Available from the National Technical Information Service, U. S. Department of Commerce, Springfield, Virginia 22161.

Price: Printed Copy A03
Microfiche A01

Codes are used for pricing all publications. The code is determined by the number of pages in the publication. Information pertaining to the pricing codes can be found in the current issues of the following publications, which are generally available in most libraries: *Energy Research Abstracts (ERA); Government Reports Announcements* and Index (*GRA* and I); *Scientific and Technical Abstract Reports (STAR);* and publication NTIS-PR-360 available from NTIS at the above address.

DOE/LC/10650-T1
(DE84006251)
Distribution Category UC-91

THE OXIDATION/GASIFICATION OF CARBON RESIDUE ON RETORTED OIL SHALE

A Final Report

Submitted to

Department of Energy

(Contract # DE-AT20-81LC10650)

by

William J. Thomson
Department of Chemical Engineering
Washington State University
Pullman, WA 99164

January 16, 1984

SUMMARY

Studies of the oxidation and gasification of oil shale char have been extended to an investigation of the effects of mineral catalysis. Six shales with differring mineral compositions were studied, including samples from the saline zone in the Western Colorado and from the Antrim shales of Michigan. Oxidation kinetics data, corrected for mass transfer effects, were compared for all six samples. A high assay shale from Utah and a sample from the saline zone were found to have the highest oxidation rates. By examining the data for shales which were water leached and thermally pretreated, it was concluded that both NaO and CaO act as oxidation catalysts.

However, as a result of mineral decomposition experiments conducted with a sample from the C-a lease tract, it appears as though the ankeritic dolomite fraction will not decompose as long as there is a minimal CO_2 over pressure. Rather, low temperature silication reactions appear to take place once the temperature exceeds 925K.

An extensive evaluation was also completed for the gasification of an Antrim shale from Michigan. Both the rates of CO_2 and steam gasification of the char were found to be markedly lower than that observed for a shale sample from the Parachute Creek member in Colorado. However, unlike the Colorado shale, the make gas resulting from the steam gasification of the Antrim shale produced nearly equal quantities of CO and CO_2. Thus, despite the high concentration of iron in the Antrim shale, the water gas shift reaction is not catalyzed nearly to the same extent as in western shales.

TABLE OF CONTENTS

INTRODUCTION

Over the past 6 years the principal investigator in this research endeavor has been involved in studies of the occurrence and associated kinetics of oil shale char reactions. There has been and remains a high motivation for studies of these reactions because of the fact that as Dockter [1] has pointed out, there is more than enough energy in the residual char remaining on retorted oil shale than is required to supply the process heat for the retorting process itself. Our initial study [2] focused on the combustion and steam gasification kinetics of a shale sample from the Parachute Creek member. Not only did this study produce useable reaction rate expressions for this oil shale, but it also pointed out the importance and uniqueness of the various mineral species with respect to their catalytic activity for those reactions. With these results the research was extended to consider other oil shales with differring mineral compositions in an effort to determine whether char oxidation/gasification reaction rates would be substantially altered in the presence of differring mineral compositions. This report deals with the results of that extended research effort.

At the time this research was initiated it appeared that study of shales found in Utah and Wyoming as well as samples from the Antrim shale deposits in Michigan would be all that was necessary in order to achieve the goals of the research. However, very early in the project it was discovered that a number of other oil shale samples had even more unusual mineral compositions and was far more deserving of study. Not only did the oil samples which were actually studied differ from that originally planned, but as the course of the research progressed,

it became apparent that focusing on the oil shale char reactions themselves would be fruitless unless a greater understanding was obtained of the mineral reactions. In addition it soon became apparent that quantitative analyses of the various oil shales was extremely important and there was very little information regarding the quantitative composition of western oil shales. Even more significantly it was not clear exactly how to best proceed with an accurate and precise quantification of the mineral composition of western oil shales. Thus the original research was altered to include a more rigorous quantification of the mineral compositions of selected oil shales and to focus on some of the mineral changes and reactions which occur during conditions typical of char oxidations/gasification. As a result of this change in direction a kinetic study of the steam gasification of these various shale samples was not undertaken. Rather, a more thorough investigation was undertaken in order to determine the specific minerals (and their compositions) which result in catalysis of the char reactions. It was found that this was achieved much more readily by concentrating on the combustion reactions of various shales since we had already developed this technique to a far greater extent. Furthermore the combustion reactions proceed at temperatures which are lower than those at which the mineral species react.

In addition to a rather complete study of the effect of minerals on char combustion, a number of experimental techniques were also developed in order to obtain a better appreciation of the extent and occurrence of the important mineral reactions. In combination with this approach, it was also decided to obtain experimental measurements of the reaction rates of some specific mineral reactions since they

occur simultaneously with residual oil shale char oxidation/gasification.

This report will discuss the experimental equipment and techniques which were used during the course of the research (some of which had to be developed) and provides a thorough discussion of some of the results. The chapter dealing with the results of the research will discuss the characterization results as well as the combustion rates of western shale and the associated effects of mineral catalysis. In conjunction with that particular phase of the project, an analytical technique will be described which was necessary to account for gas-solid mass transfer effects during oil shale char combustion in a TGA-GC apparatus. This will be followed by a presentation of the quantitative measurements of some of the important mineral reactions which act as precursors to the catalysis of oil shale char oxidation/gasification. Finally, results will also be presented for the CO_2 gasification Antrim oil shale and some semi-quantitative results of the steam gasification of that oil shale.

EXPERIMENTAL EQUIPMENT AND TECHNIQUES

Description of Shales

Six oil shale samples were selected for evaluation and comparison: one from the Parachute Creek Member (PCM), one from a deep core sample of the C-a tract (C-a), two from the saline zone in western Colorado (S-A & S-B), one from the Geokinetics site in eastern Utah (GEOK) and one sample of Antrim shale from Michigan (ANT). All of the shale samples were retorted in master batches and under identical conditions in a 2.5 cm diameter fixed bed retort. A nitrogen sweep gas at 100 scc/min was employed and the temperature was elevated at a rate of 5 K/min to a maximum temperature of 785 K at which point it was held for 1 hour.

Equipment

Figure 1 shows a schematic sketch of the experimental equipment which was used throughout the research project. Approximately 1.5 grams of spent shale (particle size approximately 100 microns) were placed in a 400 mesh stainless steel basket which was suspended from a recording electrobalance. This provided continuous gravimetric readings as the reactions proceeded. The reactor vessel was constructed of 310 stainless steel and placed in a furnace capable of reaching temperatures as high as 1200K. Any single gas or mixture of gases could be metered to the reactor via a 3.2 millimeter sparge tube and provisions were made to sample the exit gases with on line gas chromatography. This latter feature differs from most TGA apparatus which typically use extremely small sample sizes. We were forced to use a relatively large sample size in order to produce enough product gases so that measurements could be made on the gas chromatograph. In

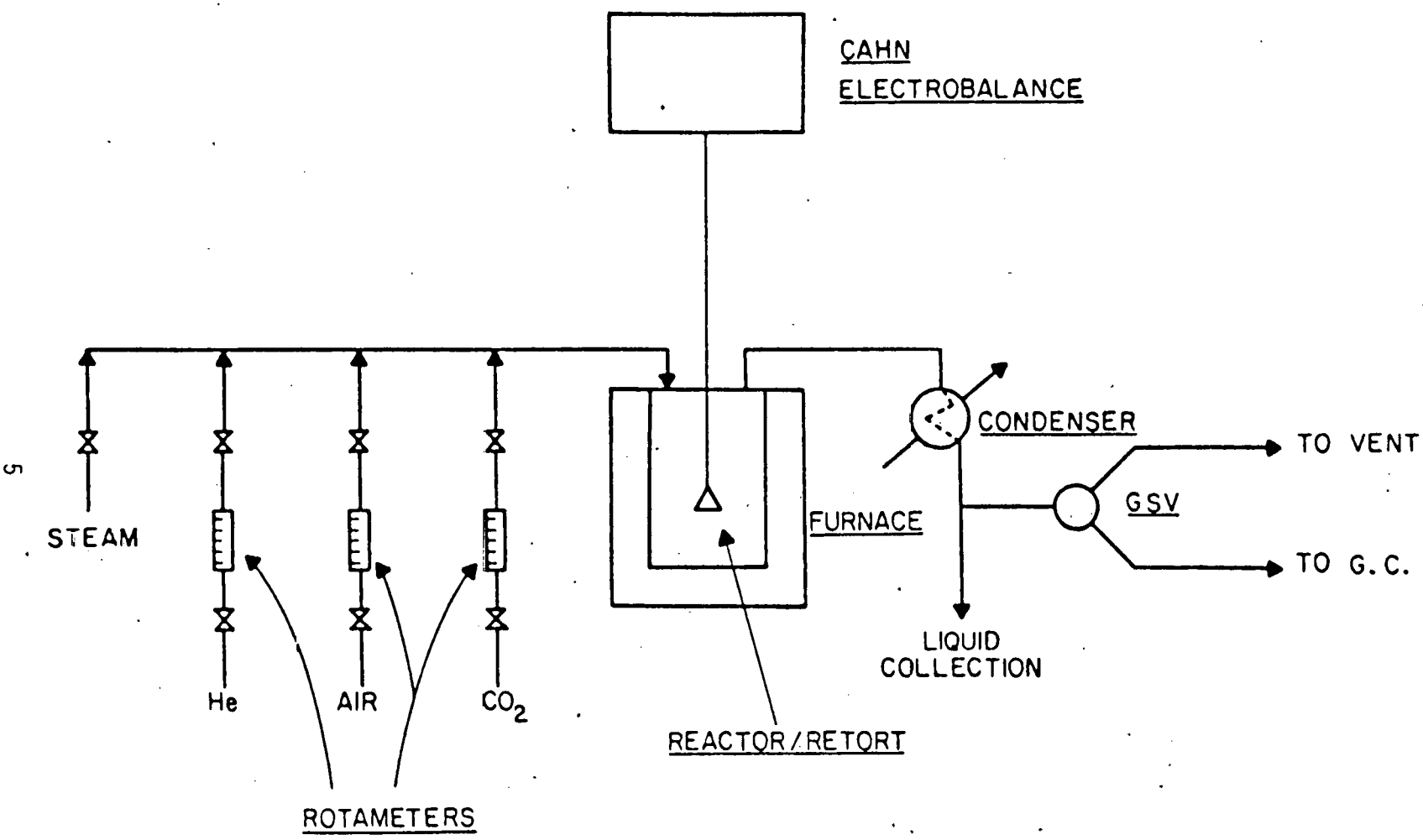

EQUIPMENT SCHEMATIC

FIGURE 1

order to insure that diffusional resistances within the shale sample bed were minimized, the shale was carefully spread over the basket in a relatively thin layer (approximately 0.4 millimeters). Worst-case diffusional calculations indicated that diffusion resistance could be safely neglected and this was verified when experiments with half loadings gave the same results as those with full 1.5 gram loadings. The reactor had a diameter of 10 centimeters and a total volume of 1100 cubic centimeters. Two shielded chromel-alumel thermocouples were placed near the shale sample. One thermocouple was placed two centimeters above the sample and the other was placed so that it barely missed touching the sample itself. The latter thermocouple was used to monitor temperature excursions during the initial stages of combustion. The temperature differences between these two thermocouples rarely exceeded 10 K and then only for one or two minutes.

While the TGA-GC system just described was the primary experimental equipment used in this research, selected shale samples were also analyzed via various electron microscope/microprobe apparati. Use was also made of the Department of Geology's X-ray florescence unit (for elemental composition data) and of the X-ray diffraction apparatus at DOE's facility in Laramie, Wyoming. In addition, a number of the samples were subjected to acid leaching in order to quantify the percentage of mineral carbonates present in the shale. Some of the samples were also leached in water as well as in acid and in both cases the leachate waters were analyzed by the Department of Chemical Engineering's atomic absorption apparatus.

Procedures

Depending on the phase of the research being conducted, different procedures were followed and these were critically important to the

carrying out of the experimental research plan. First of all with respect to the combustion studies, the samples were first heated to the desired temperature in a helium atmosphere in order to remove adsorbed moisture. Once the weight trace on the TGA-GC stabilized, the desired concentration of oxygen was selected by diluting air with helium. A number of the experiments were conducted in the presence of undecomposed carbonates and in these cases the temperatures were never allowed to exceed 800K. In some cases the samples were first subjected to high temperatures (800-1050K) in either a helium or CO_2 atmosphere in order to effect changes in the mineral compositions. Once that goal had been obtained the sample was then cooled to the desired combustion temperature and exposed to the pre-selected oxygen concentration. In other cases the samples were first water leached or acid leached in order to extract mineral carbonates and/or soluble sodium salts. Prior to the combustion tests themselves, these samples were first dried in an inert atmosphere at 575K and then the procedure just described was followed.

All of the shale samples studied in this investigation were first grossly characterized with respect to their mineral content by allowing them to decompose in a helium atmosphere as the temperatures were raised from 800K to 1200K at a heating rate of 2.7K/min. As mentioned earlier, two of the shale samples were selected for a more thorough investigation of their mineral reaction activity. In these experiments the samples were first "decharred" under mild oxidation conditions (10 percent O_2, 700K). Since the primary methods of analysis involved TGA techniques, it was important to attempt to isolate the various mineral reactions so that some guarantee could be obtained that we were looking

at individual reactions and not simultaneous reactions. As will be discussed in the Results section of this report this was not always possible. The procedures and ensuing problems are best understood by referring to the three sets of reactions which describe the primary mineral reactions occurring: the decomposition of ankeritic dolomite (Equation (1)), the reversible decomposition of calcite (Equation (2)), and the formation of silicates from calcite (Equation (3)).

$$CaMg_xFe_{1-x}(CO_3)_2 \rightarrow CaO + xMgO + (1-x)\,FeO + 2CO_2 \qquad (1)$$

$$CaCO_3 \rightleftharpoons CaO + CO_2 \qquad (2)$$

$$CaCO_3 + MgO + SiO_2 \rightarrow CaMg\ Silicates + CO_2 \qquad (3)$$

In all samples the presence of CO_2 could prevent calcite decomposition because of the reversible natures of (2). However, of the two samples studied in this phase of the project (C-a and PCM), it was found that the ankeritic dolomite in the C-a sample would not decompose (Equation 1) below 925 K in the presence of CO_2. This minimum temperature for ankeritic dolomite decomposition was very close to the range where silication reactions were expected. Therefore, it was first necessary to study the silication reactions (Equation (3)) by raising the sample to the desired temperature (1000-1150 K) in the presence of CO_2. Ankeritic dolomite decomposition was investigated by measuring the decomposition rates of virgin samples in a CO_2-free environment at temperatures between 800 K and 925 K. Reversible calcite decomposition was then studied by recarbonating the CaO formed in Equation (1) and varying the CO_2 pressures as well as temperature.

In our earlier work with the gasification of the PCM shale, it was found to be necessary to first decompose the shale to calcium oxide in

order to prevent calcite decomposition from occurring simultaneously. Since in the work reported here we concentrated on the Antrim shale and this shale is extremely low in mineral carbonates (see discussion under Results), we were able to prepare the sample for CO_2 and steam gasification by first allowing it to decompose in an inert helium atmosphere at a temperature of 1100 K. During this preliminary preparation we were surprised to find that there was a slow but steady decomposition reaction which occurs. However the rates were so low that it was not possible to measure anything in the offgas except for a very small quantity of CO_2 which we suspect is being produced by the relatively slow decomposition of a sideritic mineral. Another possibility is that it is due to the high temperature decomposition of very stable clays which would be expected to give off water and which could not be detected with the equipment used in our study.

RESULTS

Shale Characterization

As discussed earlier, all six shale samples were subject to X-ray diffraction (XRD) analyses, X-ray florescence analyses (XRF), and acid leaching. In addition the oil yield during the retorting was measured and is reported as gallons per ton (note that this is not a Fisher assay procedure). The retorted shale was then submitted for CHN analyses and this in turn was used to calculate the percentage of organic carbon on the spent shale. As anyone versed in the field of mineral analyses is aware, it is extremely difficult to obtain precise quantitative information on mineral composition. With this in mind the results shown in Tables I and II should not be viewed with anymore precision than $\pm$ 20%. Table I shows the quantity of oil collected during retorting, the percentage of organic carbon on the spent shale and the percentage of some of the more important elements obtained by XRF. Although there is a wide variation in the oil yields, we have previously shown [3] there to be no effect of assay on the combustion activity of the spent shale. However, it is interesting to note that the GEOK spent shale sample had over twice the organic carbon content of the PCM sample even though the two had similar oil yields. This could indicate that the original kerogen in the GEOK sample was more aromatic than that in the PCM sample [4]. The other parameter which varies significantly from shale to shale is the percentage of calcium present in the spent shale. As can be seen, it ranges from a high of 15.2% in the GEOK sample to a low of 0.7 percent in the ANT sample from Michigan. It is also noteworthy to point out the difference in the calcium content between the S-A and S-B sample. The S-A sample has 8 times the quantity of calcium as the S-B sample and 7 times the sodium content.

TABLE I

COMPOSITION OF SPENT SHALE SAMPLES

			WGT % SPENT SHALE						
SAMPLE	GPT[a]	C[b]	Ca	Mg	Fe	Al	Na	K	Si
PCM	50	5.1	10.2	3.4	2.8	5.0	2.6	1.7	18.8
C-a	25	3.5	12.3	3.5	2.5	4.3	2.0	1.7	16.2
GEOK	44	11.9	15.2	4.3	3.1	4.8	2.3	2.0	19.6
S-A	30	3.8	8.4	3.6	3.1	6.3	2.8	2.1	22.3
S-B	40	3.9	1.0	1.0	5.6	10.9	0.4	1.7	30.2
ANT	11	7.0	0.7	1.2	5.4	8.3	0.4	3.4	31.0

[a] Gallons per ton

[b] Organic carbon

TABLE II

Mineral and Elemental compositions

	WGT. % SPENT SHALE				
Minerals	GEOK	C-a	S-A	S-B	ANT
Ankerite	43	35	28	0	0
Dolomite	0	0	4	0	0
Kutnohorite-Mg	0	18	0	0	0
Calcite	19	20	7	7	0
Quartz	14	8	9	24	23
Pyrite	0	0	0	0	5
Pyrrhotite	5	0	20	6	6
Siderite	0	0	0	0	6
Albite	10	10	23	31	23
Microcline	0	0	6	0	0
Illite	3	0	0	6	13
Other	6	9	3	20	24
Elemental					
Ca	15.2	12.3	8.4	1.0	.07
Mg	4.3	3.5	3.6	1.0	1.2
Fe	3.1	2.5	3.1	5.6	5.4
Al	4.8	4.3	6.3	10.9	8.3
Na	2.3	2.0	2.8	0.4	0.4
K	2.0	1.7	2.1	1.7	3.4
Si	19.6	16.2	22.3	30.2	31.0

The S-A sample is from the saline zone in Colorado and is known to be high in nahcolite and dawsonite. Another piece of data to be pointed out is the fact that although the iron contents are roughly the same in all of these samples they are slightly higher in the S-B and the ANT samples. Iron is typically found in spent shale in the form of ankeritic dolomite, pyrite, pyrrhotite and siderite. It is interesting that in viewing the mineral compositions reported in Table II (as reported by DOE'S X-ray diffraction measurements), that the percentage of pyrrhotite in the S-B and ANT samples is significantly lower than that in the S-A sample even though the former had a higher iron content. As a result it is difficult to rationalize the percentage of pyrrhotite shown for the S-A sample. In comparing the S-B and ANT mineral analyses, the ANT sample would appear to have substantially higher iron than the S-B sample. This arises from the fact that it contains 5% Pyrite, 6% Pyrrhotite and 6% Siderite. The 6% value for siderite is consistent with some of the high temperature decomposition reactions discussed earlier. It is also interesting to observe that pyrite was found only in the ANT sample. It is thought that during retorting pyrite reacts with the hydrogen given off during the pyrolsis of kerogen to form pyrrhotite. This explains the absence of pyrite in the other four samples and the fact that all but the C-a sample contain substantial quantities of pyrrhotite. It is possible that since the ANT sample is known to be high in sulphur and the kerogen is low in hydrogen, that all of the pyrite was not converted to pyrrhotite during retorting. Again, this discussion points to the difficulty in attaching quantitative significance to X-ray diffraction results in the absence of an internal standard.

Figure 2 is another method of illustrating the effects of carbonate minerals in the various shale samples. As can be seen this figure shows the mass loss for the spent shales as the temperature was raised linerarly at 2.7°K/min. in a helium purge stream. In the GEOK sample, only one large mass loss is apparent and this occurs at about 600°C. This is attributed to dolomite/calcite decomposition and is consistent with the relatively high percentage of calcium present in this shale (see Table I). There are two distinct mass loss occurrences with the ANT sample: one at 500° C and the other at 625°C. These are attributed to clay minerals which are typically found in devonian shale. The comparison between S-A and S-B is very interesting since there appears to be much less mineral decomposition in the S-B sample. Again this is qualitatively consistent with the mineral composition results shown in Table II where none of the mineral carbonates (ankerite, dolomite, kutnohorite) were detected. However, the fact that this sample did experience an additional weight loss of 3% at temperatures above 550°C points to the fact that there must indeed have been some mineral carbonates present in the shale despite the mineral analysis. The weight loss behavior for the S-A sample shows an increase in the mass loss rate at 480°C and then another at about 620°C. The former is attributed to dawsonite decomposition and the loss at 620°C is attributed to calcite decomposition.

Interpretation Of Kinetic Data From TGA Experiments

Whereas TGA techniques have desirable and unique properties when it comes to the analysis of the rates of solid reactions which are accompanied by weight changes, there are also a number of deficiencies associated with this technique. For one, depending upon the size of the sample utilized, high sweep gas flow rates can cause severe

FIGURE 2

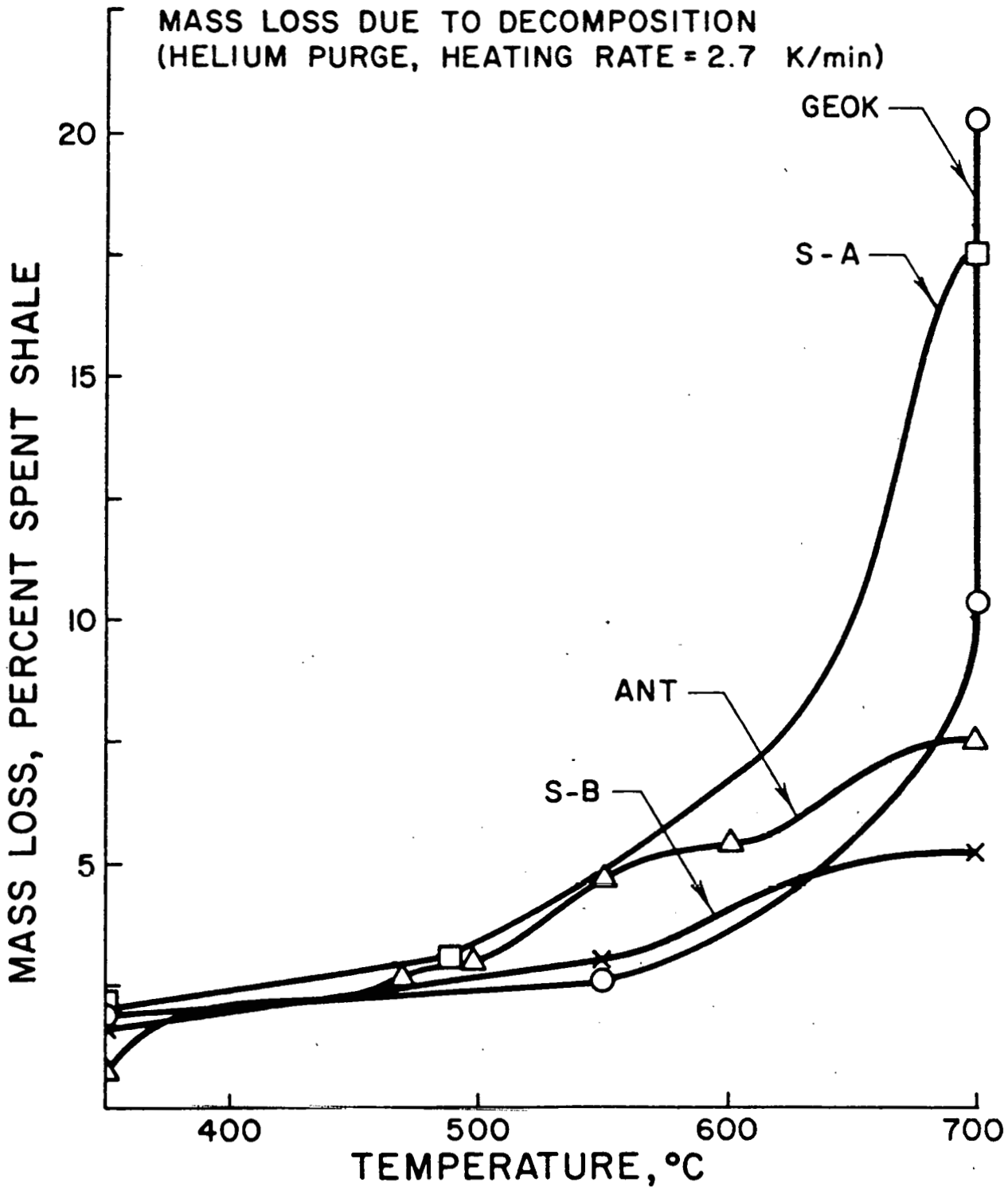
MASS LOSS DUE TO DECOMPOSITION
(HELIUM PURGE, HEATING RATE = 2.7 K/min)
GEOK
S-A
ANT
S-B
MASS LOSS, PERCENT SPENT SHALE
20
15
10
5
400
500
600
700
TEMPERATURE, °C

oscillations in the gravimetric weight trace and lower the ultimate sensitivity of the technique itself. Unfortunately, in the case of high solid reaction rates (such as combustion) high sweep gas rates are desirable in order to minimize gas-solid mass transfer limitations. During the course of this investigation we discovered that the char combustion activities were unusually high and, consequently, mass transfer limitations played a significant role, particularly at the higher temperatures. Trial and error experimentation indicated that we could not eliminate the mass transfer resistance by simply raising the sweep gas flow rate due to unacceptable oscillations in the gravimetric readings. Consequently, it was decided to attempt to model the behavior of char combustion in our TGA apparatus and thereby account for the mass transfer resistances separately.

Still another problem was associated with the fact that at time = zero, a desired oxygen or steam concentration was selected and fed to the reactor. Even in the absence of the reacting solid there is a finite amount of time required before the reactor itself will reach the inlet concentration of the reacting gas. Since our reactor system behaved as an ideal backmix reactor, this is easily accounted for by standard tracer techniques and these have already been conducted and described in an earlier publication [3]. However, in the case of a reacting sample the problem is aggravated by the fact that the reactant gas is consumed during the reaction at the same time that it is attempting to fill the reactor to the desired concentration. Again, the only recourse here was to model the TGA apparatus and thereby simultaneously account for the mixing phenomenon in the CSTR along with the reaction occurring on the solid surface.

Assuming ideal back mixing, an unsteady state material balance for the gaseous reactant, 'A', gives

$$\frac{dC_A}{dt} = \frac{1}{\tau} (C_{A_i} - C_A) - M_s r_G \qquad (4)$$

where τ is the space time, C_{A_i} is the feed gas concentration, M_s is the solid sample mass and r_G is the global rate of reaction expressed on a per unit mass basis. Assuming that the reaction is first order with respect to both A and the solid species, 'B', r_G is given by

$$r_G = k_{AP} C_A C_B \qquad (5)$$

where the apparent rate constant, k_{AP} accounts for both the mass transfer (k_M) and kinetic (k) rate coefficients

$$k_{AP} = \frac{k}{1 + \frac{kC_B}{k_m A_g}} \qquad (6)$$

where A_g is the surface area of the exposed solid surface per unit of mass. A similar balance on the solid species yields

$$\frac{dC_B}{dt} = - k_{AP} C_A C_B \qquad (7)$$

Another potential problem is that, due to the highly exothermic nature of the combustion, the actual solid temperature may be higher than the surrounding gas temperature. This can be accounted for by taking an energy balance on the solid, assuming that the gas temperature remains constant at T.

$$C_p \frac{dT_s}{dt} = (- \Delta H) r_G + hA_g (T - T_s) \qquad (8)$$

where T_s is the solid temperature and C_p, ΔH, and h are the heat capacity, the heat of reaction and the heat transfer coefficient respectively.

Equations 4-8 were solved simultaneously using an equation-oriented dynamic simulation program. All of the non-reaction parameters were known with the exception of the heat and mass transfer coefficients. The heat transfer coefficient was determined by comparing the predictions of the computer-simulation to measured surface temperature responses of a sample during an actual combustion run. Similarly, the mass transfer rate coefficient was determined by comparing the predictions of the program to an actual experiment which was obviously controlled by gas-solid mass transfer rates. The only other assumption in this model was that the reaction be first-order with respect to both the gaseous and solid reactants. Fortunately, this turned out to be the case and the successful comparison of the model predictions with actual experimental data validated this assumption.

To illustrate the success of this approach, Figure 3 shows the char combustion data for the GEOK sample. Note that the higher temperature data do not follow a straight line on a first-order plot. The fact that the lowest temperature run did follow a straight line and that the low conversion data are similar at all temperatures is a clear indication of mass transfer problems. The downward trend of the high conversion data is due to the shifting of the char reaction order from 0 (mass transfer control) to 1 (kinetic control). As can be seen from equation (6), the apparent rate constant is a function of the concentration of the solid species (C_B) at any time. Thus initially,

FIGURE 3

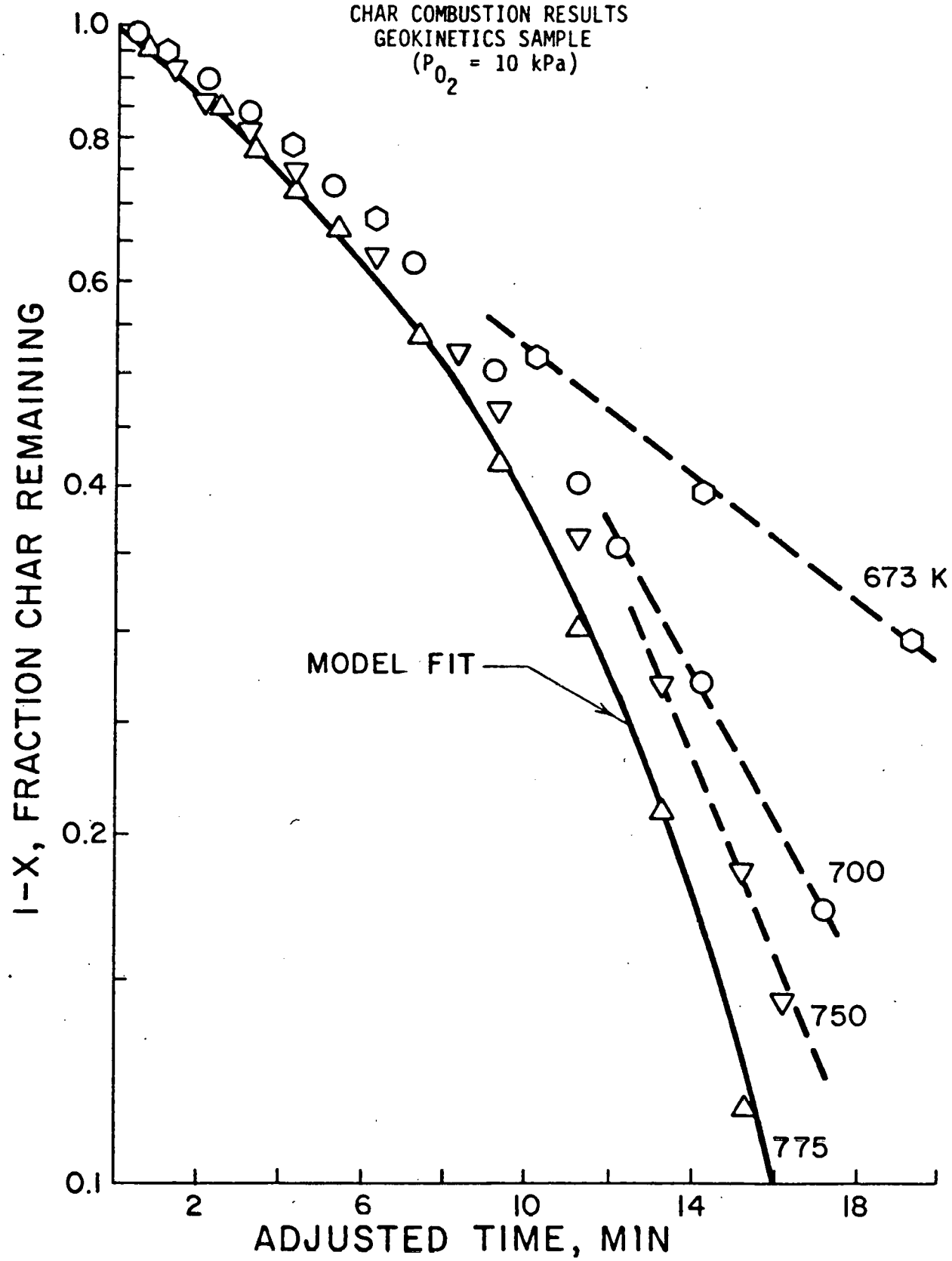
CHAR COMBUSTION RESULTS
GEOKINETICS SAMPLE
(P_{O_2} = 10 kPa)
1.0
0.8
0.6
0.4
0.2
0.1
I-X, FRACTION CHAR REMAINING
MODEL FIT
673 K
700
750
775
2
6
10
14
18
ADJUSTED TIME, MIN

when C_B is high, the apparent rate constant is inversely proportional to C_B and the rate (equation 5) becomes zero order with respect to species B. Note that in this case the apparent rate constant is close to the mass transfer rate coefficient. What is more, late in the run when C_B is low, the apparent rate constant approaches the kinetic rate constant, k. In this case, equation (5) predicts that the global rate will be first-order with respect to both species A and species B. As can be seen from Figure 3, the model gives an excellent prediction of both the low and high conversion data for the run at 775 K. Similar results were obtained at the other temperatures (not shown) and for all the shale samples utilized in this investigation.

Char Combustion Kinetics

As in our earlier work [5] the combustion reaction rate was found to be first order with respect to both O_2 and char content. Table III lists the apparent rate constants in terms of the pre-exponential factor and the activation energy for all six samples as well as comparative values at 700 K. The S-A sample had the highest activity and has high concentrations of dawsonite and nahcolite. Although these minerals will have decomposed prior to combustion, the decomposition products (Na_2CO_3, Al_2O_3) are present and, as will be shown, there is strong evidence to indicate that the sodium acts as a catalyst. It is also interesting that the activation energies are lowest for the two shales (S-A and GEOK) with the highest rate constants. It is tempting to attribute this result to catalytic influences of the mineral matter but, at these temperatures (<800K) the carbonate minerals are still in their original state and there is no evidence to suggest that they are catalytic under these conditions. Char combustion kinetics have been

TABLE III

KINETIC PARAMETERS

$$k = ko\,EXP\left[\frac{-E}{RT}\right] \quad (kPa\text{-}min)^{-1}$$

SAMPLE	$ko \times 10^{-5}$	E^a	k (700K)
PCM	2.45	97.07	.0140
C-a	8760.	142.3	.0212
GEOK	11.51	91.21	.0236
S-A	.002	49.79	.0385
S-B	.480	93.72	.0049
ANT	5.42	104.8	.0082

a KJ/mol

previously reported for Antrim shale by Rostam-Abadi and Mickelson [6]. In that study the authors reported that the rate was second order with respect to the char remaining and that there was noticeable chemisorption of O_2. Attempts to fit our data for the Antrim shale to a second order rate expression were unsuccessful and, in all cases, the data appeared to follow first order kinetics. Although we did not have the precision to measure O_2 chemisorption, that phenomenon is consistent with our previous observations [5] of catalytic activity in those shales containing decomposed mineral carbonates. That is, the catalytic activity of CaO was attributed to its ability to chemisorb O_2. As will be discussed in more detail below, the Antrim shale sample did not contain such carbonates and no catalytic behavior was observed. However, the magnitude of the rate constants reported by Rostam-Abadi and Mickelson are very similar to those measured here.

Finally it should be pointed out that the pre-exponential factor listed in Table III for the PCM sample, differs from the value we reported earlier [5]. From our measurements of the actual shale temperatures we have discovered that the measured temperatures in the earlier study were in error. The values listed in Table II are now consistent with the reported measurements of Sohn and Kim [7].

Mineral Catalysis

The mineral reactions that accompany high temperature char combustion have already been listed in equations (1-3). Although we made no effort to study the reaction rates of these mineral reactions in detail, it is important to understand just how fast these reactions are under typical temperature-gas composition conditions. For example, in some earlier work [2] we found that equation (1) would go to the "half-calcined" state when CO_2 is present. That is, only 1 molecule of

CO_2 would be given off and calcium carbonate rather than calcium oxide would be a product. However, in the case of the C-a shale we discovered that this mineral carbonate remained undecomposed even in the presence of slight CO_2 overpressures (7 KPA). That result was noted at a temperature of 850 K but when the temperature was raised to approximately 925 K, a noticeable weight loss was observed on our TGA apparatus. We have tentatively concluded that in this shale, ankeritic dolomite will not decompose in the presence of CO_2; but at the relatively low temperature of 925 K it will undergo low temperature silication reactions of the form shown in equation (3). In another sample (GEOK sample) the shale was allowed to undergo partial silication and then the sample was ground and polished and subjected to electron microprobe analysis. The results of this analysis are shown in Figure 4 which shows a line scan traverse across a 10 grain of silica. As can be seen, there is virtually no calcium present in the inner regions of the silica grain and no silica present beyond the outer surface of the grain. However, there is a distinct shell of approximately one-half micron thick which consists of both calcium and silica. Obviously a silicate layer is forming around a silica grain. This is significant since, as will be discussed below, the oxide decomposition products are those species which we believe to be responsible for char combustion catalysis. If silicates are formed such as shown in Figure 4, then catalytic activity will not result and could have a significant influence on the design of suitable char combustors.

While these two mineral reactions are important, it is reversible calcite decomposition (equation (2)) which is the most significant

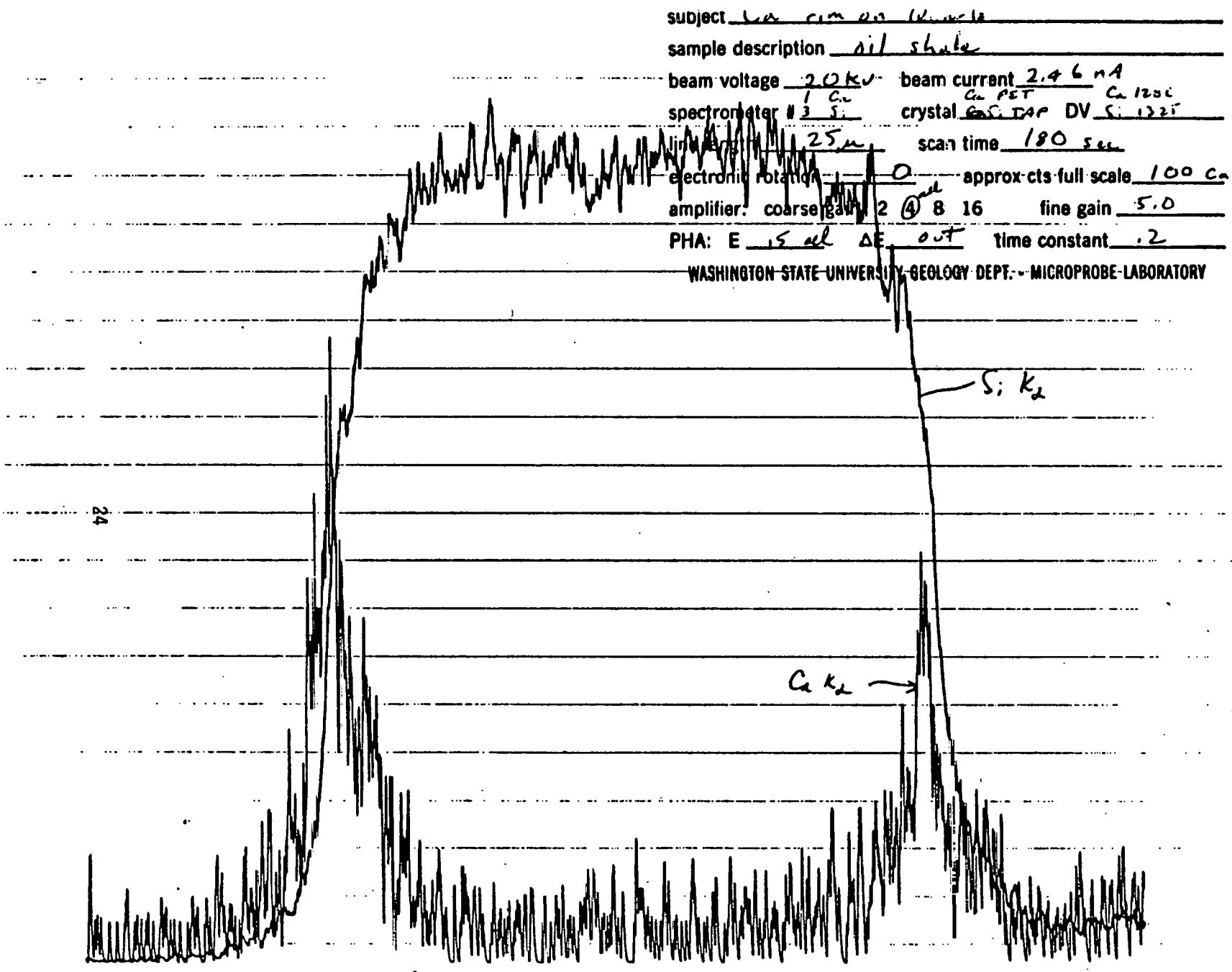

Figure 4: Electron Microprobe Line Scan Across a Partially Reacted Grain of Quartz in Oil Shale Ash

mineral reaction of interest here. Not only is the reversible nature of this reaction of importance, but all of our data point to the significant catalytic activity of the product, CaO. In an earlier experiment [5] we took a freshly retorted PCM sample and allowed it to thermally decompose at 900 K to the mineral oxides (equation (1)). When this reaction was complete, the temperature was lowered to 700 K and the sample exposed to oxygen. Under these conditions the observed combustion rate was 10 times higher than when the carbonates were left intact; i.e., corresponding to the kinetic results given in Table III. By process of elimination, the increased activity in this case was attributed to the presence of CaO. In order to further investigate this phenomenon, the same experiment was carried out with the C-a and with the ANT sample. The C-a sample was chosen due to the fact that it contained more calcium than char on a molar basis. On the other hand, the ANT sample had a very low calcium content, and as we have already seen in Figure 2, it was very low in mineral carbonates.

Figure 5 shows the comparative responses of the raw thermogravimetric readings when the decomposed samples were exposed to 10% O_2 at time = zero. Similar behavior was observed for the C-a and PCM samples; that is, the raw weight increased due to the recarbonation of CaO.

$$C + O_2 \longrightarrow CO_2 \qquad (9)$$

$$CaO + CO_2 \longleftarrow CaCO_3 \qquad (10)$$

Since the combustion rate is at least as fast as the recarbonation rate, the data in Figure 5 correspond to a combustion rate increase of about an order of magnitude in both samples. It should be pointed out that the weight change in PCM reached a maximum and then decreased due

Figure 5

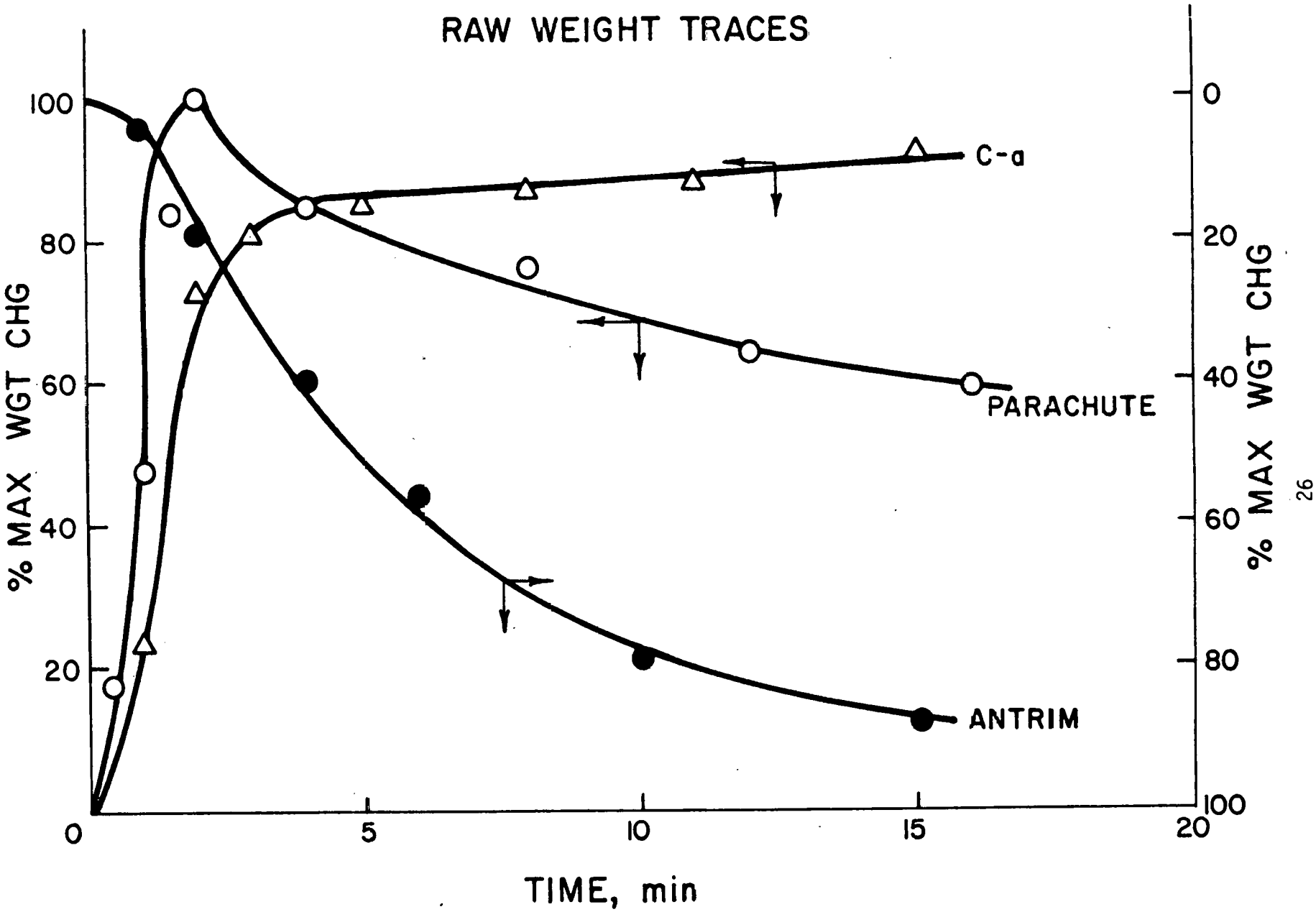
RAW WEIGHT TRACES
% MAX WGT CHG
100
80
60
40
20
0
0
20
40
60
80
100
% MAX WGT CHG
C-a
PARACHUTE
ANTRIM
0
5
10
15
20
TIME, min

to the total recarbonation of the available CaO prior to complete combustion of the char. This was not the case for C-a which has more CaO than char. It is also interesting to note that the ANT sample, which has minimal Ca, did not experience a weight gain during combustion. In fact, the combustion rate was identical to that observed for ANT samples which had not been thermally pretreated. These results tend to support the hypothesis of CaO as a combustion catalyst. Although iron oxides cannot be totally ruled out, it should be noted that the ANT sample is very high in iron (most of it as FeS and FeS_2 but some as iron oxide) but exhibited no catalytic activity.

Additional experiments were also run in order to examine the effects of water soluble mineral species on the combustion rate. Figure 6 shows first order plots for one S-B and two S-A samples. As pointed out earlier, the S-A and S-B samples are similar except for high concentrations of nahcolite and dawsonite in the former and it is this sample, which had the highest combustion activity (Table III). Since it is possible to water leach sodium minerals, the S-A sample was subject to water washing prior to combustion. After drying, the sample was combusted under identical conditions and, as can be seen from Figure 6, the combustion rate for the water washed S-A sample was identical to that observed with the S-B sample. In order to determine the elements removed during the water leaching process, the wash-water was analyzed using atomic absorption. Table IV shows the results of these analyses for the S-A sample as well as for the S-B and GEOK samples. As expected, the S-A leachate was extremely high in Na. The fact that neither Ca nor Fe was leached from the S-A sample and that the GEOK sample showed no change in combustion rate despite similar potassium values points to the probable role of Na as an oxidation

Figure 6

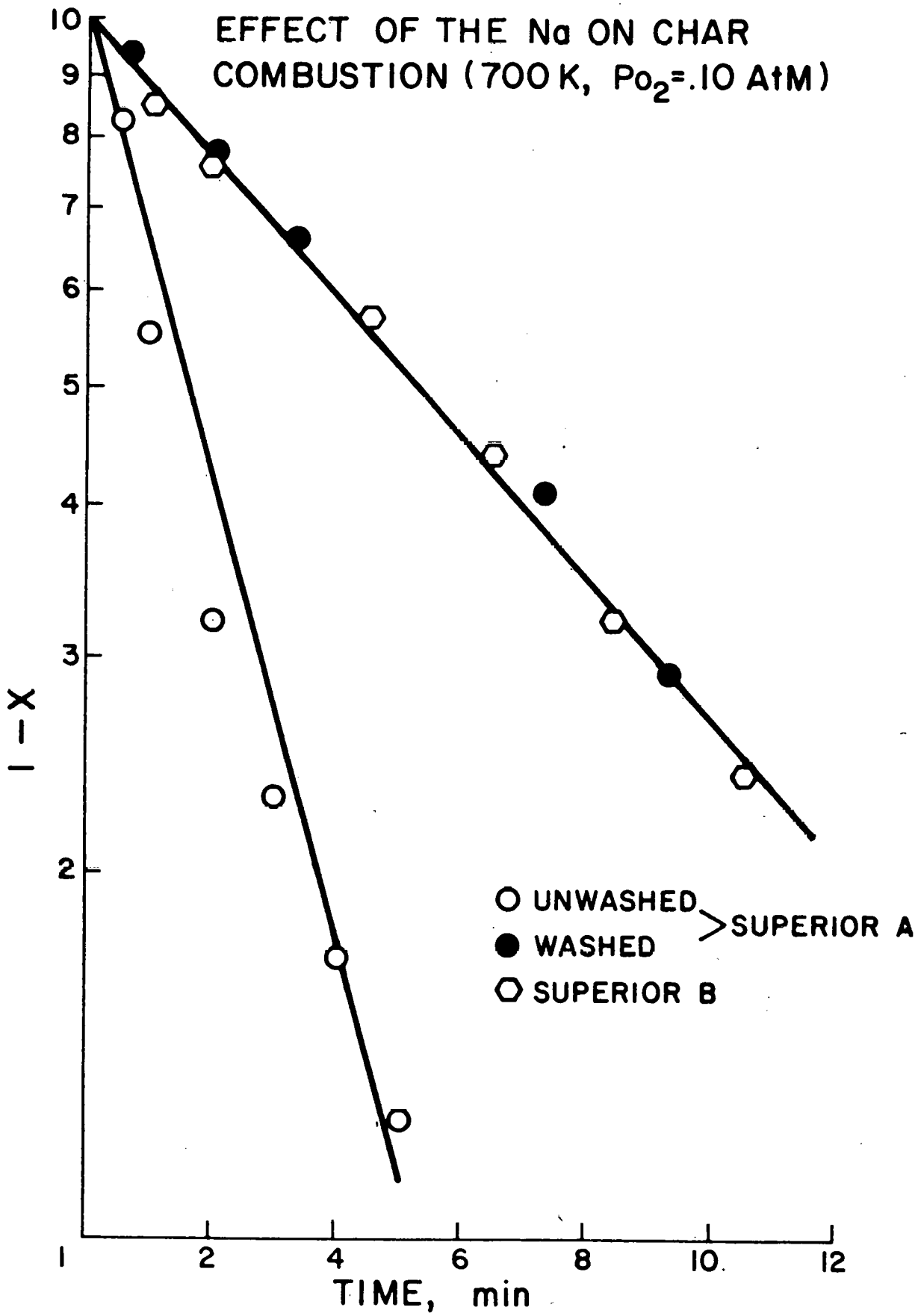
EFFECT OF THE Na ON CHAR COMBUSTION (700 K, Po_2=.10 AtM)
10
9
8
7
6
5
4
3
2
1 - X
1
2
4
6
8
10
12
TIME, min
UNWASHED
WASHED
SUPERIOR B
SUPERIOR A

catalyst. This is not too surprising since it is well known that the Group I-a and, to a lesser extent, Group II-a elements are good gasification catalysts [8].

Table IV. Elemental Analysis of Leachate Water

Concentrations - mg/g Spent Shale

SHALE	Na	K	Ca	Fe
S-A	21.7	0.24	0.0	0.0
S-B	0.15	0.05	0.49	0.0
GEOK	0.93	0.23	1.90	0.0

Antrim Shale Gasification

One of the complexities involved in studying antrim shale gasification by TGA techniques is the necessity to quantify accompanying mineral reactions. To achieve this, a sample of decharred antrim shale was heated in a helium sweep gas and the mineral reactions were monitored by weight loss and chromatographic analysis of the off-gas. Figure 7 shows these results in the form of an Arrhenius plot. Although there is some data scatter, it appears that there are two distinct reactions, one occurring between 800K and 1000K, and the second at temperatures greater than 1000K. The only gaseous species present at the lower temperatures is CO_2 but it is not present at the higher temperature. It is likely that the lower temperature reaction is a mineral decomposition (perhaps siderite decomposition) but the source of the weight loss at the higher temperatures has not been identified.

Because of the unexpected mineral decomposition reaction(s), we were not able to rely on gravimetric methods alone to determine the

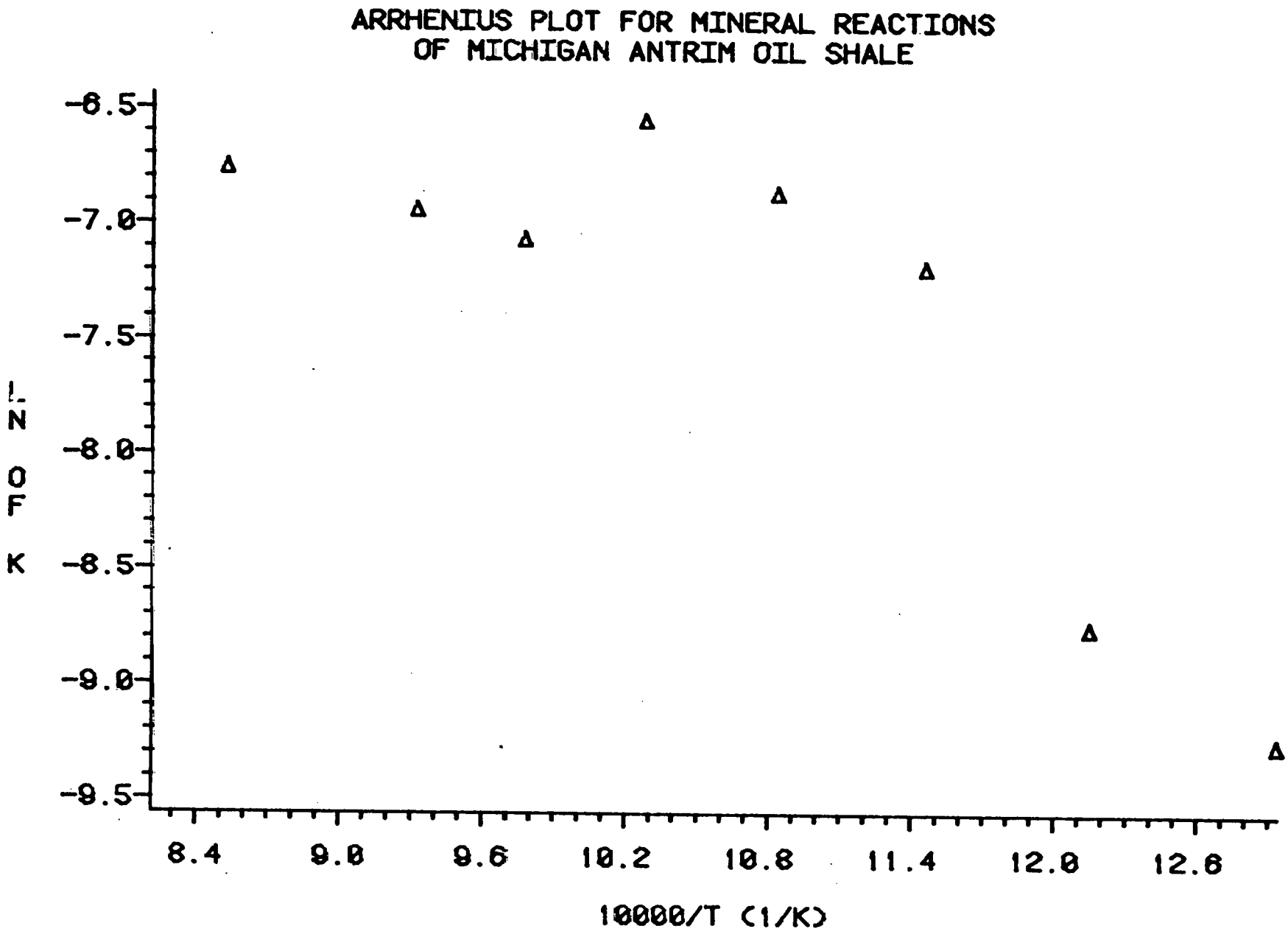
ARRHENIUS PLOT FOR MINERAL REACTIONS
OF MICHIGAN ANTRIM OIL SHALE
-6.5
-7.0
-7.5
-8.0
-8.5
-9.0
-9.5
LN OF K
8.4
9.0
9.6
10.2
10.8
11.4
12.0
12.6
10000/T (1/K)

FIGURE 7

char gasification rates. Thus, in the case of CO_2 gasification we also monitored the rate of production of CO, since this can be related to char consumption by equation (11).

$$CO_2 + C \rightleftharpoons 2CO \qquad (11)$$

In the case of steam gasification, two reactions were expected to be significant

$$H_2O + C \longrightarrow CO + H_2 \qquad (12)$$

$$H_2O + CO \rightleftharpoons CO_2 + H_2 \qquad (13)$$

Since both CO and CO_2 could be expected in the exit gas stream, the char consumption rate was determined by calculating the molar production rate of carbon in the exit gas (by measurements of the gas composition and the gas flow rate). When these calculations were compared to measured weight losses and corrected for mineral decomposition (Figure 7), agreement to within 10% was achieved.

CO_2 Gasification

Measureable CO_2 gasification began at about 1000 K and was reasonably fast at 1250 K. Figure 8 shows the results when the exit CO flow rate is plotted as a function of time at temperatures between 1073 and 1173 K for P_{CO_2} = .20 atm. For an ideal back mix reactor, the actual char reaction rate is related to the molar CO flow rate, $\dot{N}_{CO}$, by equation (14).

$$r_c = \frac{1}{2M_s}\left[V_R \frac{dC_{CO}}{dt} + \dot{N}_{CO}\right] \qquad (14)$$

where V_R is the reactor volume and M_S is the mass of the shale loading.

It is interesting to compare these results with those measured earlier [9] for a western shale from the Parachute Creek member (PCM

FIGURE 8:

CO_2 Gasification Results (P_{CO_2} = 0.20 atm)

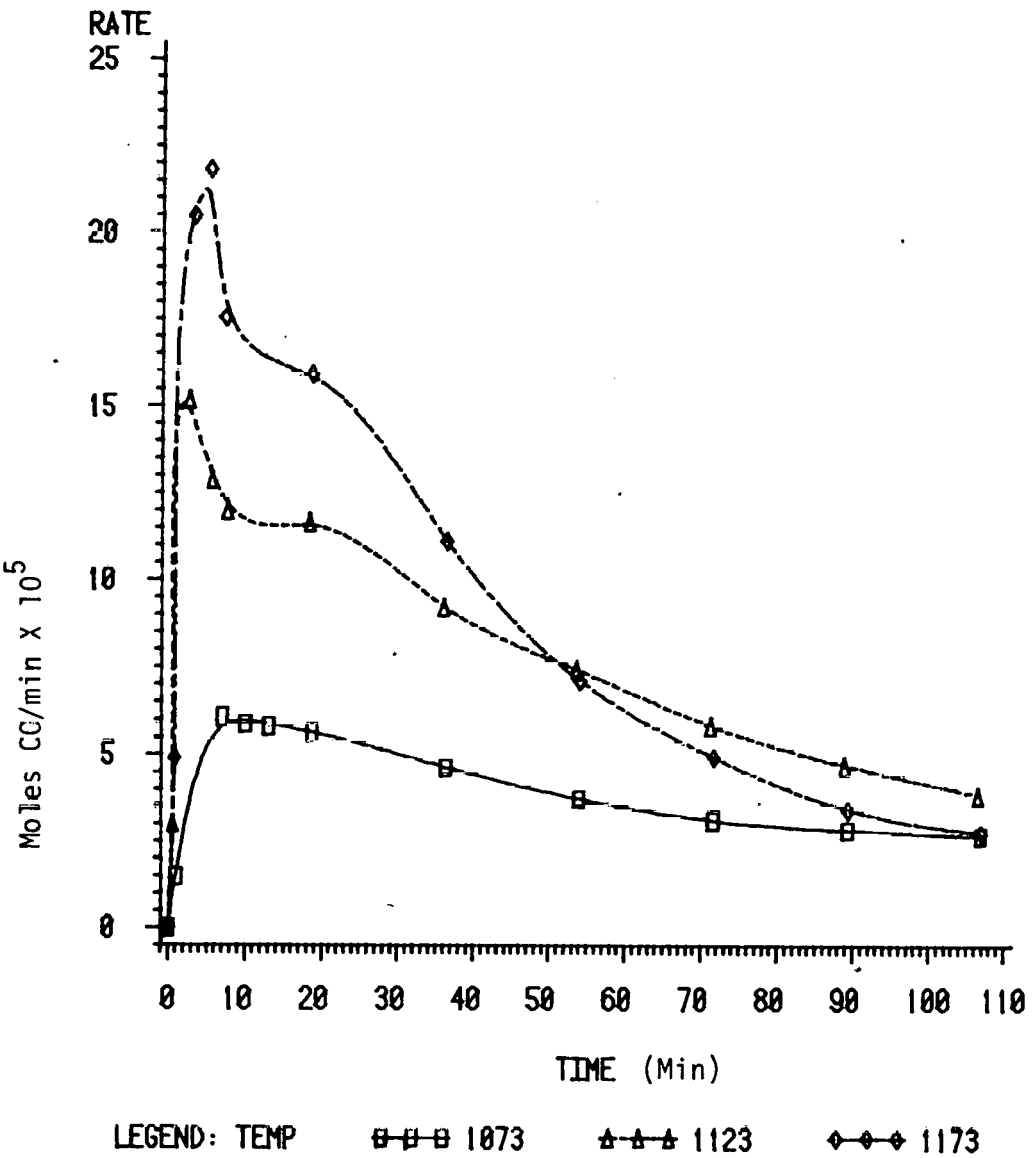

sample). Such a comparison is shown in Table V and, as can be seen, the gasification rates here are about a factor of five lower at 1073 K

TABLE V

Comparison of CO_2 Gasification Rates

Temp.	r_c (mole char/min-g shale) X10^3					
	1073 K			1173 K		
P_{CO_2} (atm)	.10	.20	.30	.10	.20	.30
ANT	.032	.035	.091	.11	.15	--
PCM	.167	.251	.302	.98	1.5	--

and a factor of about 10 lower at 1173K. This indicates that the activation energy for CO_2 gasification is lower for the ANT shale. The fact that there also seems to be less of a dependence on CO_2 pressure for the ANT sample, might be indicative of increased adsorption inhibition by the CO_2 product.

Steam Gasification

In the case of steam gasification there are two factors which are of importance; the rate of char comsumption and the composition of the make gas. With respect to the former, Table VI shows the char gasification rates for both the ANT sample investigated here and the PCM sample [9].

TABLE VI

Comparison Of Steam Gasification Rates

[P_{H_2O} = 0.5 atm]

	r_c (moles char/min - g shale) X 10^4	
	1123 K	1173 K
ANT	2.2	3.7
PCM	8.8	13.2

Here again the ANT sample has a lower gasification rate although it appears that, in steam gasification, the activation energies are similar.

However the make-gas composition was dramatically different from that reported earlier [2] for the PCM sample. Over a wide range of pressures and temperatures, the quantity of CO produced with the PCM shale was extremely low. This was attributed to the tendency of the PCM shale to promote the water gas shift reaction (WGSR), equation (13). That is, as soon as the CO is formed by the gasification reaction (equation (12), it immediately reacted with excess H_2O to produce CO_2 and H_2.

That this is not the case here can be seen in Figure 9 and 10 which show the make-gas composition at 1123 and 1173 K for P_{H_2O} = 0.5 atm. At the lower temperature (Figure 9), the CO/CO_2 ratio is about unity throughout the run. In the PCM sample, it was consistently less than 0.10, particularly at P_{H_2O} values greater than 0.2 atmospheres. However, at the higher temperature, the CO/CO_2 ratio is less than 1.0 although the rate of production of both CO and CO_2 increases significantly. If all of the H_2 produced results from the steam gasification of the char, it should agree with

FIGURE 9:
Make Gas Composition at 1123 K
(P_{H_2O} = 0.5 atm)

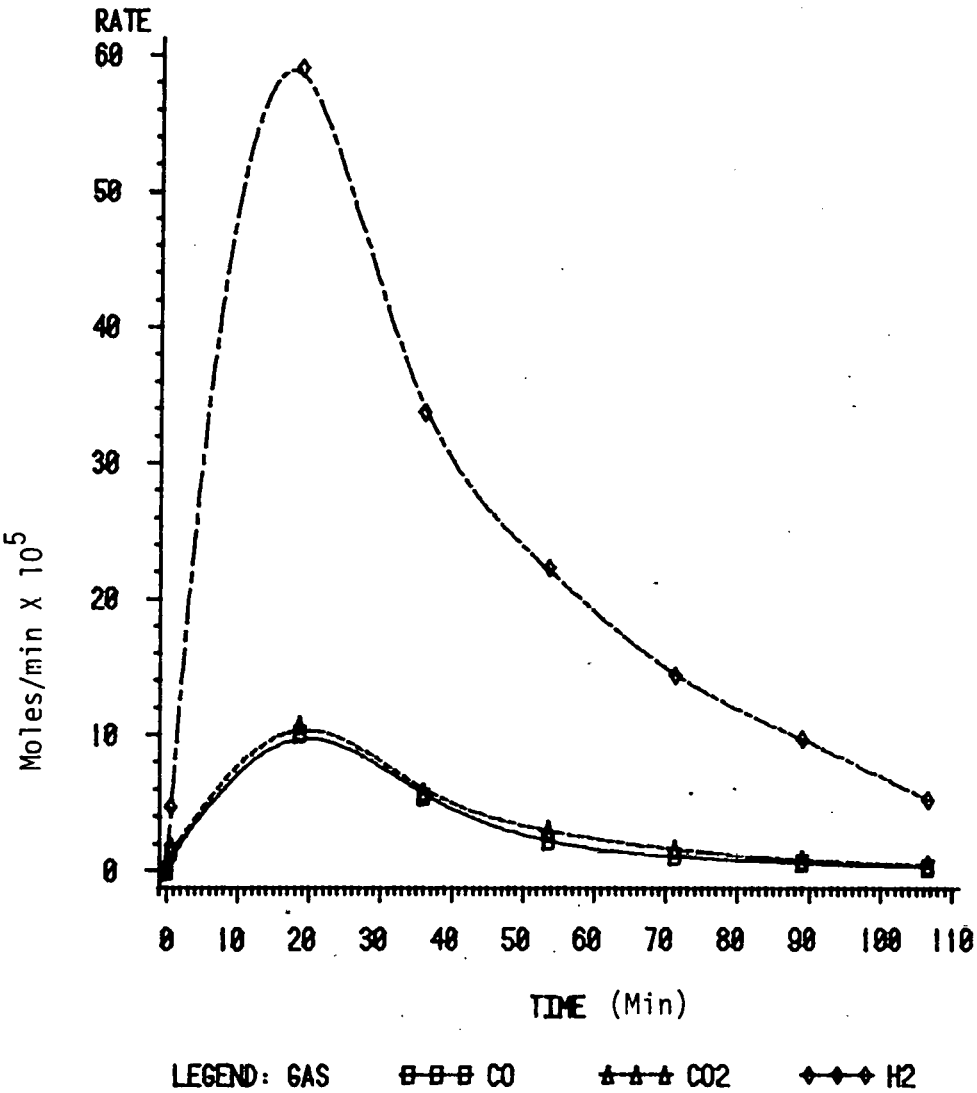

FIGURE 10:

Make Gas Composition At 1173 K

(P_{H_2O} = 0.5 atm)

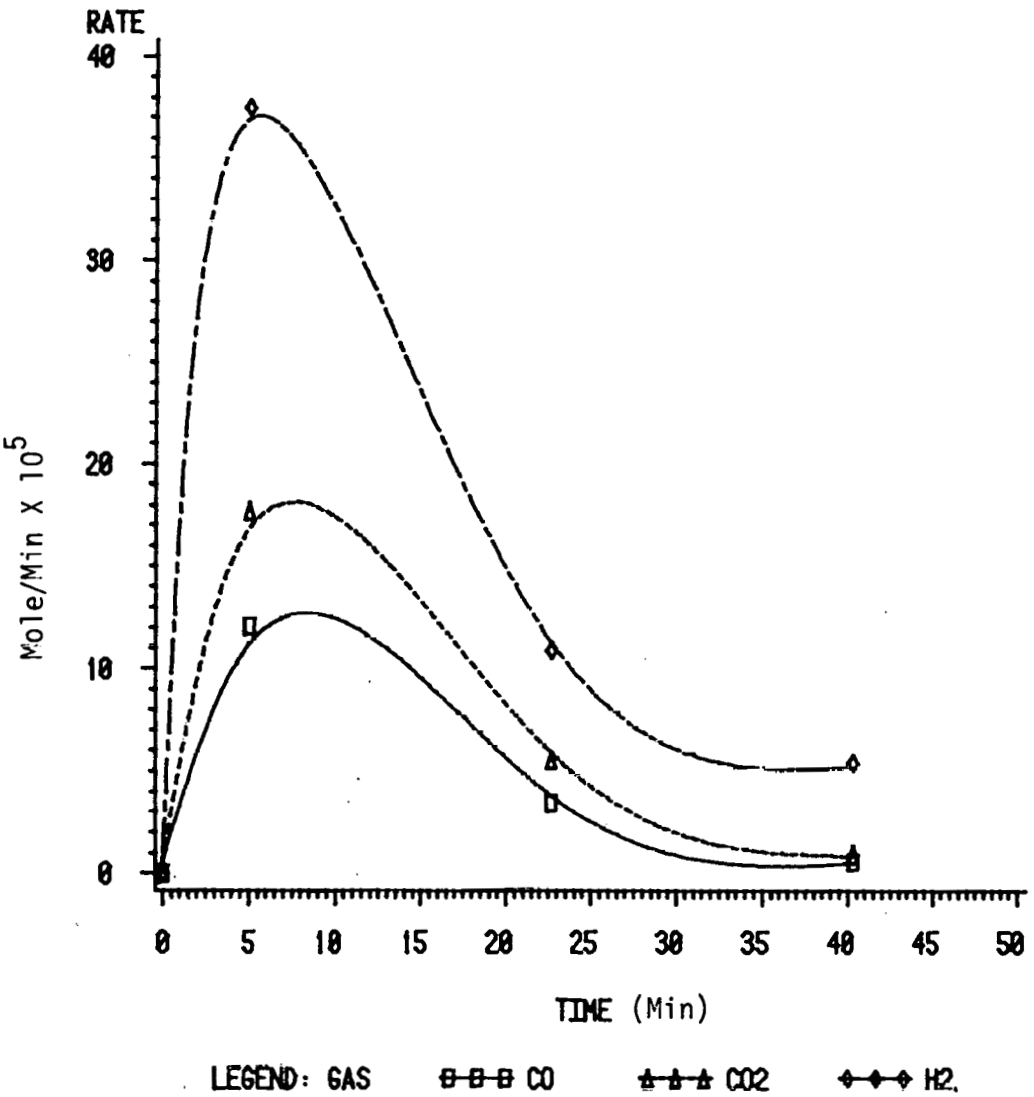

$$\dot{N}_{H_2} = \dot{N}_{CO} + 2\,\dot{N}_{CO_2} \qquad (15)$$

Thus, at 1123 K it should have a peak value of about 30 X 10^{-5} moles/min. However, the data shown in Figure 9 indicate that $\dot{N}_{H_2}$ is consistently twice what would be predicted by equation (15). A goodly portion of this difference arises from the hydrogen contained in the char. In addition, it is likely that the pyrrhotite is reacting with the steam to produce iron oxides, H_2S and, perhaps, additional H_2.

At the higher temperature (Figure 10), the hydrogen make is <u>less</u> than that calculated from equation (15). As can be seen from Figure 11, which shows the hydrogen production rate for the two temperatures, the rate is dramatically reduced at 1173 K. The explanation here is that much of the H_2 being produced is undergoing further reaction to reduce pyrrhotite and produce H_2S. This was verified by measuring the H_2S in the exit gas and noting the increase at 1173 K versus 1123 K. Thus, if steam gasification can be accomplished at a reasonable rate at lower temperatures, it appears as though H_2S production can be minimized.

FIGURE 11:

H_2 Make Gas

(P_{H_2O} = 0.5 atm)

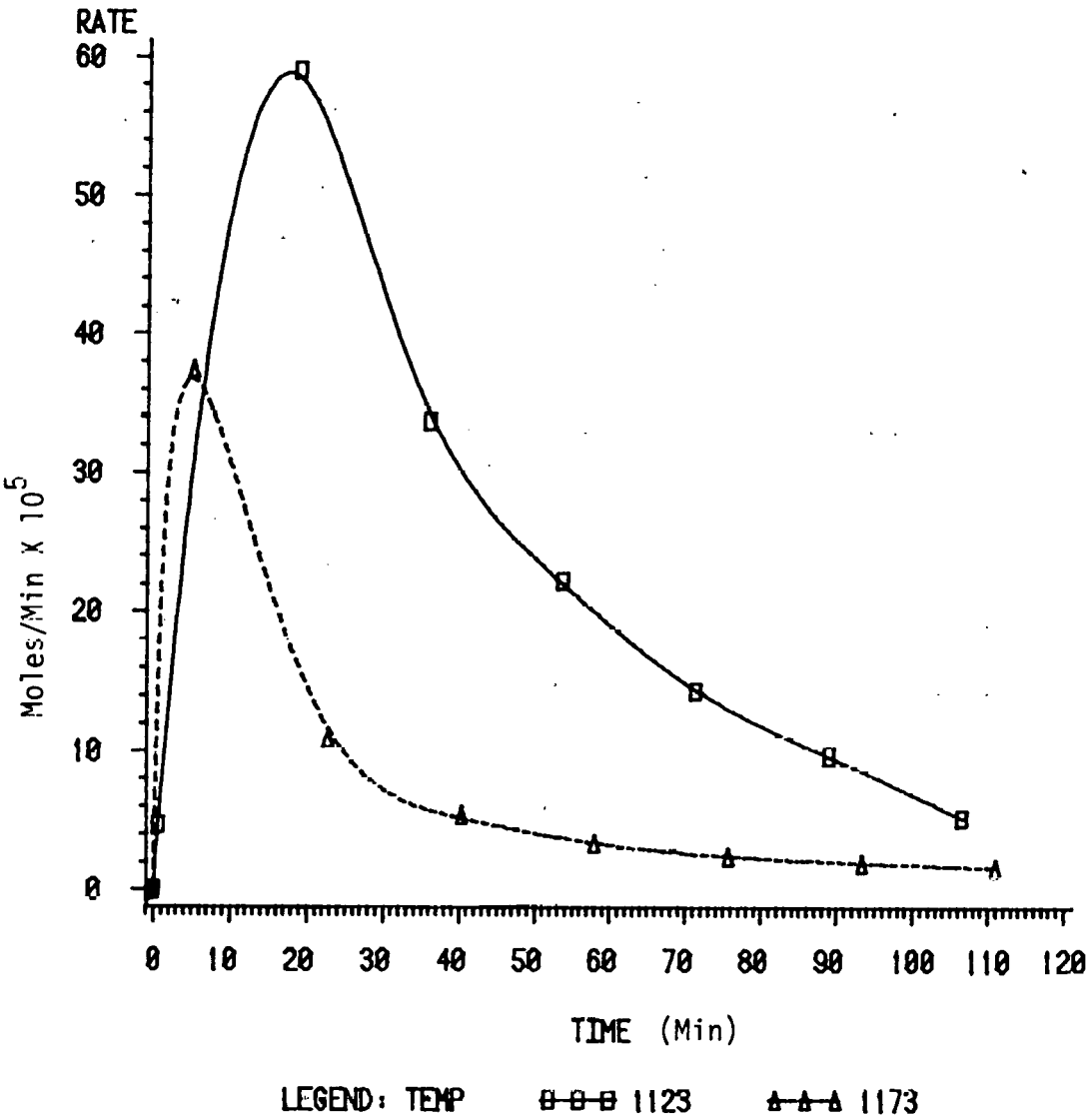

REFERENCES

[1] Dockter, L., paper presented at 68th Annual Meeting of AIChE, Los Angeles, Nov. 20 (1975).

[2] Thomson, W. J., "The Oxidation/Gasification of Retorted Oil Shale", report submitted to DOE, Contract No. DE-A507-77ET12099, Oct. (1979).

[3] Soni, Y. and Thomson, W. J., Proc. 11th Oil Shale Symp., p 364, (1978).

[4] Rubel, A. M. and T. T. Coburn. 1981. Influence of Retorting Parameters on Oil Yield from Sunbury and Ohio Shales from Northeastern Kentucky. Proceedings of the 1981 Eastern Oil Shale Symposium. pp.21-28.

[5] Soni, Y. and Thomson, W. J., I & EC Proc. Des. & Dev., 18, p 661 (1979).

[6] Rostam - Abadi, M. & Mickelson. R. W., paper presented at National AIChE Meeting, Anaheim, June 7 - 10 (1982).

[7] Sohn, H. Y. and Kim, S. K., I & EC Proc. Des. & Dev., 19, p 550 (1980).

[8] Wen, W. Y., Catal. Rev. - Sci. Eng., 22, p 1 (1980).

[9] Thomson, W. J., Gerber, M. A., Hatter, M. A. and Oakes, D. G., ACS Symp. Ser., No. 163, p 115 (1981).

☆U.S. GOVERNMENT PRINTING OFFICE: 1983-746-081/2569